Spatial Chaos

1985 Phys. Scr. 1985 64

(http://iopscience.iop.org/1402-4896/1985/T9/009)

Physica Scripta. Vol. T9, 64–69, 1985

Spatial Chaos

Mogens Høgh Jensen

H.C. Ørsted Institute, Universitetsparken 5, DK-2100 Copenhagen Ø, Denmark

and

Per Bak

Physics Department, Brookhaven National Laboratory, Upton, New York 11973, USA

Received August 3, 1984; accepted August 5, 1984

Abstract

Spatial chaos may arise as a consequence of competing spatial periodicities just as temporal chaos may be caused by competing temporal periodicities or frequencies. In particular, spatial chaos occurs in condensed matter systems where one of the periods is that of the crystal lattice, and the other period that of a modulated ordered structure. As an example we review recent results on an axial Ising model where the chaotic states appear as trajectories of a four-dimensional map.

1. Introduction

Most of the lectures at this symposium have been devoted to the phenomenon of chaos in dynamical systems, or "chaos in time". In particular, temporal chaos appears as a consequence of resonance effects between two competing frequencies [1].

An analog situation exists in systems with two spatial periods, where the competition can lead to "chaos in space". The mathematical formulation is very similar in the two cases. In dynamical systems the chaotic behaviour is usually described in terms of discrete maps which relate the state of the system at some instant to the state at a previous time. In the second case the state of the system at some spatial position (for instance a lattice site in a condensed matter system) is related to the state of the system at another position through a discrete map. For instance, the equilibrium states of the "Frenkel–Kontorowa" model of an array of atoms, connected with springs, in a periodic potential can be found among the solutions to Chirikovs standard map [2, 3], and some of these solutions are chaotic with positive spatial Lyapunov exponent. The chaos is spontaneous in the sense that there is no quenced disorder or "external noise" in the model, in contrast to spin glasses where the chaos is induced by spatial disorder.

As a specific example of a system, which exhibits spatial chaos, we shall consider an Ising model with competing nearest and next-nearest neighbor interactions, the ANNNI model [4–6]. The model has ordered phases with modulated structures as shown schematically in Fig. 1. There is a non-linear coupling between the modulated structure and the lattice. This coupling gives rise to a competition between the modulation period and the lattice period which tends to lock the modulation period into a commensurate one where P modulations correspond to Q lattice periods. The wave number, or "winding number" of the commensurate structure is $q = P/Q$. The phase diagram of the ANNNI model is shown in Fig. 2. Note the tongues where the wave vector is rational. At high temperatures near the critical line separating the ordered modulated phases from the paramagnetic phase the commensurate phases do not fill up the phase diagram and there is room for incommensurate "quasi-periodic" phases between the commensurate ones [5]. At low temperatures, where the non-linear coupling is stronger, there are only commensurate phases. The two regimes are separated by a critical line which probably is fractal.

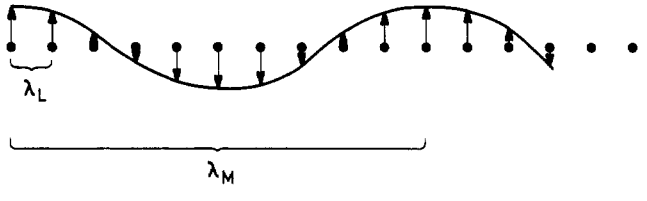

Fig. 1. Modulated structure of the ANNNI model; λ_M and λ_L denote the periodicities of the modulation and the lattice, respectively.

Figure 3 shows for comparison the phase diagram of the circle map which describes dynamical systems with competing frequencies such as the driven damped pendulum [1]. The Arnold tongues represent regimes where the frequencies are locked into rational ratios $W = P/Q$. For small values of the non-linear coupling K there is room for quasi-periodic orbits between the periodic ones. For stronger non-linearity (increase of K) all resonances increase in width and for large values of K ($K > 1$) there is zero probability of finding a quasi-periodic orbit. The similarity between the two phase diagrams is striking.

2. The ANNNI model as a discrete 4-dimensional map

In the ANNNI model, nearest neighbor spins interact through a

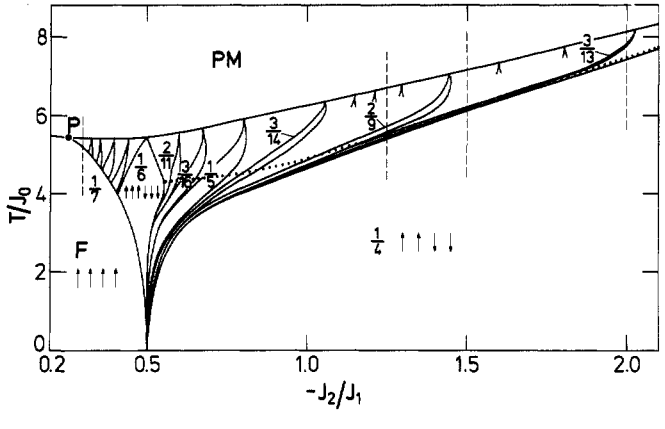

Fig. 2. Phase diagram of the ANNNI model [5, 6]. T/J_0 is the ratio between the temperature and the NN in-plane coupling. J_2/J_1 is the ratio between the NNN and the NN axial coupling.

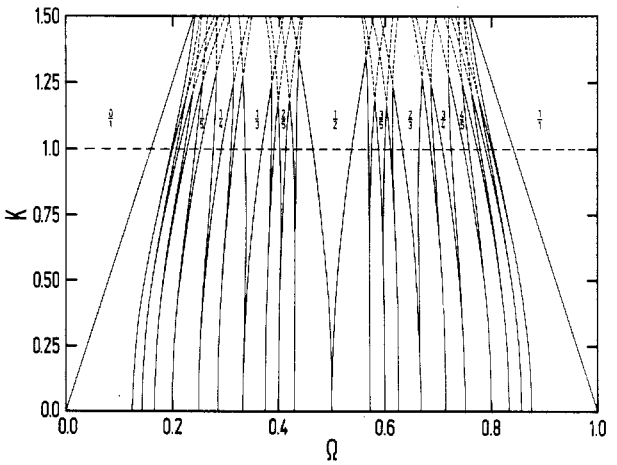

Fig. 3. Phase diagram of a dynamical system described by the circle map [1]. Note the similarity with Fig. 2.

ferromagnetic interaction J_1. In addition there is an antiferromagnetic next-nearest neighbor interaction J_2 in the "axial" direction only. The competition between J_1 and J_2 gives rise to structures which are modulated in the axial direction but uniform in the perpendicular direction.

Let $M_i = \langle S_i \rangle$ denote the magnetization of the ith layer in the axial direction. The mean field H_i acting on a spin in the ith layer is

$$H_i = (M_{i+1} + M_{i-1})J_1 + (M_{i+2} + M_{i-2})J_2 + 4M_iJ_1 . \quad (1)$$

The magnetization at the ith layer can be related to the mean field

$$M_i = \tanh \frac{H_i}{T}, \quad (2)$$

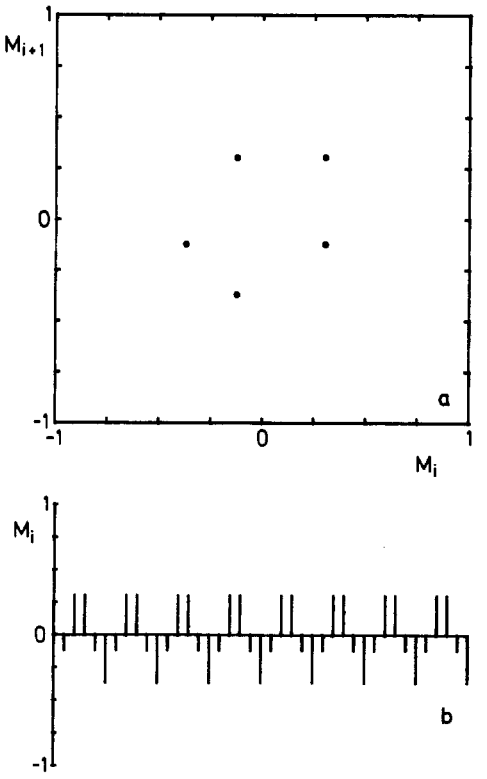

Fig. 4. Periodic solution to the 4d map and the corresponding spin structure.

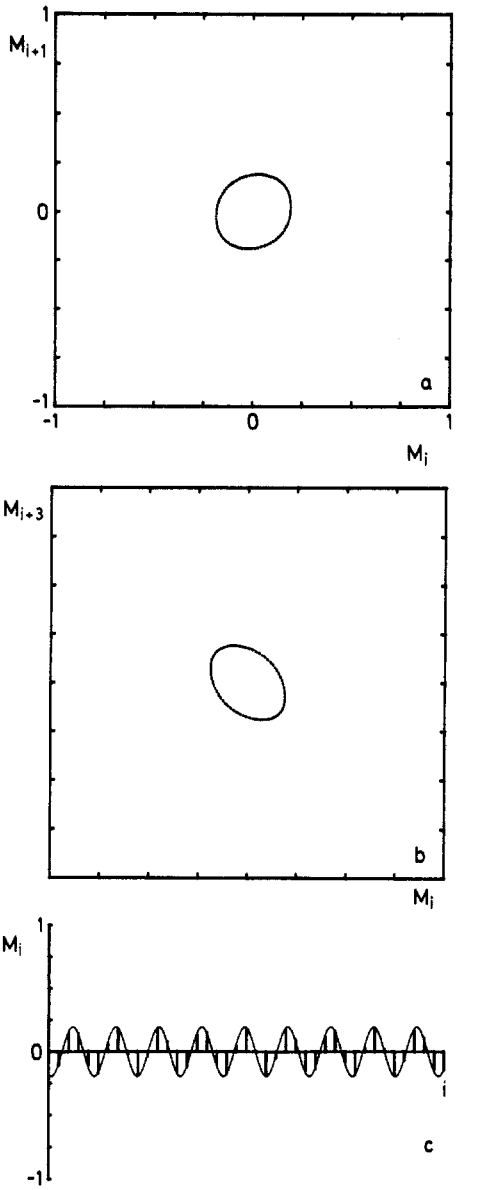

Fig. 5. Incommensurate ("quasi-periodic") solution characterized by a one-dimensional curve.

so eq. (1) can be written

$$M_{i+2} = -\frac{J_1}{J_2}(M_{i+1} + M_{i-1}) - M_{i-2} - 4\frac{J_1}{J_2}M_i + \frac{T}{J_2}\tanh^{-1} M_i$$
$$= f(M_{i+1}, M_i, M_{i-1}, M_{i-2}) \quad (3)$$

This equation defines a four-dimensional non-linear discrete map

$$T: \begin{bmatrix} M_{i-2} \\ M_{i-1} \\ M_i \\ M_{i+1} \end{bmatrix} \rightarrow \begin{bmatrix} M_{i-1} \\ M_i \\ M_{i+1} \\ M_{i+2} = f(M_{i+1}, M_i, M_{i-1}, M_{i-2}) \end{bmatrix}, \quad (4)$$

and solutions to the mean field equations can be generated by iterating the map, starting with an initial configuration with four consecutive values of the magnetization (M_1, M_2, M_3, M_4). The numerical procedures involved in determining the various equilibrium structures are described in detail in [6].

Figure 4 shows a two dimensional projection of a periodic

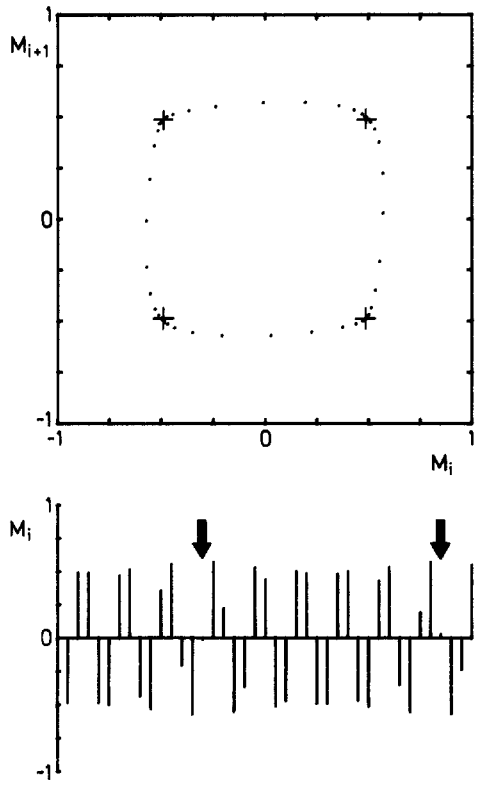

Fig. 6. Incommensurate phase near the $q = Q/P = 1/4$ commensurate phase. The solitons are marked by arrows.

"commensurate" orbit, and the corresponding spin structure with a periodicity of five lattice constants. An incommensurate structure takes in general the form

$$M_i = g(qi + \alpha) \tag{5}$$

where g is a periodic function, $g(x + 1) = g(x)$, q is an irrational wave number, and α an arbitrary phase measuring the "position" of the modulated structure. The $4d$ orbit defined by eq. (5) is

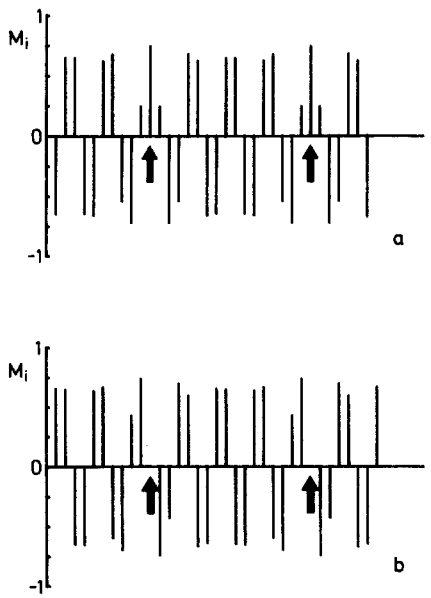

Fig. 7. "Pinned ' (a) and "depinned" (b) commensurate structures.

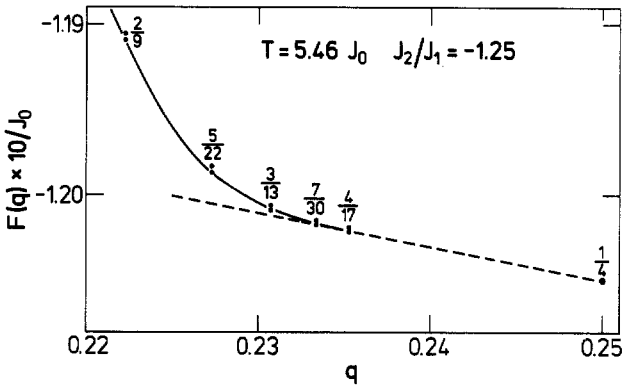

Fig. 8. Free energy per spin vs wave number at a point in the parameter space near the commensurate-incommensurate (CI) transition. The slope of the broken tangential line is negative indicating that the soliton energy in eq. (7) is positive, so the soliton-free C phase is stable. For slightly higher values of T the slope is positive and it is favorable to have a finite density of defects, so the C phase is unstable.

$$\begin{aligned}(M_{i-2}, M_{i-1}, M_i, M_{i+1}) &= (g(q(i-2)+\alpha), \ldots, g(q(i+1)+\alpha)) \\ &= (g(x), g(x+q), g(x+2q), g(x+3q)),\end{aligned} \tag{6}$$

which is a one-dimensional curve since the argument x (mod 1) ergodically assumes all values $0 < x \leqslant 1$ when q is irrational. Figure 5 shows such an incommensurate orbit generated by iterating the map, and the corresponding spin-structure.

In addition to the C and I structures the model has stable chaotic structures, which, however, cannot be ground states of the model. In order to understand how these structures arise in a natural way in the model, we approach the strong non-linear regimes (i.e. we lower the temperature) and consider first the nature of incommensurate phases near commensurate phases, and the C–I transition. Figure 6 shows an incommensurate phase near the $q = 1/4$C phase. The spin-structure takes the form of a lattice of defects, or "solitons" separating regimes with commensurate $++--++$ structure. The distance between two solitons is not an integer number of lattice constants since

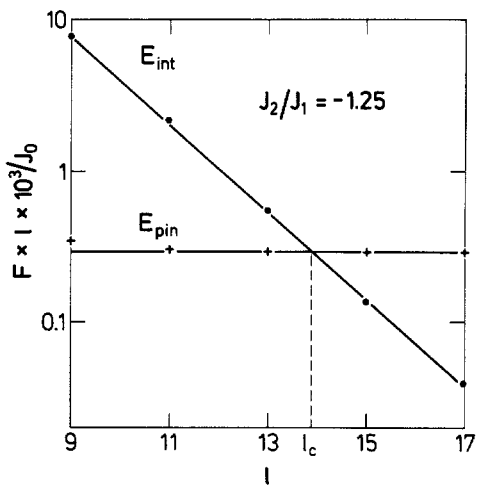

Fig. 9. Pinning energy and interaction energy vs soliton distance. $E_{\text{int}} \sim E_{\text{pin}}$ for $l_c \sim 14$.

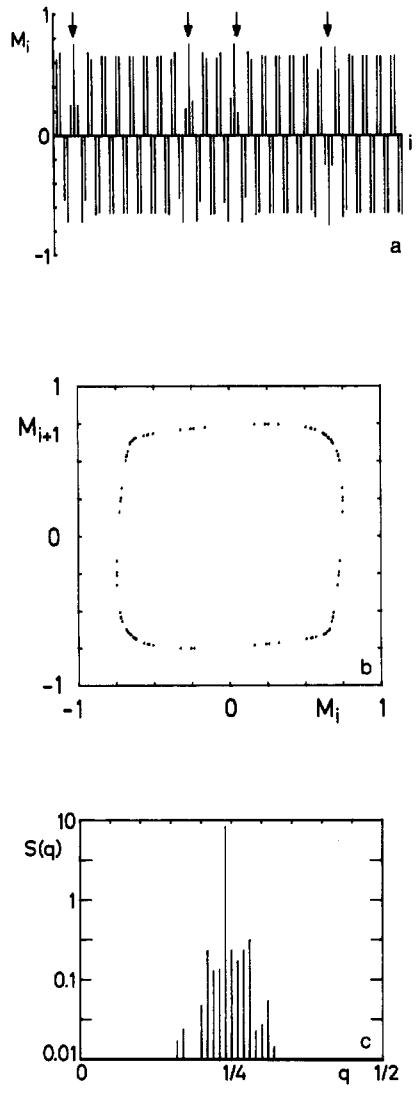

Fig. 10. Chaotic state formed by randomly pinned defects [6]. (a) spin-configuration, the solitons are marked by arrows; (b) the corresponding trajectory of the 4d map; (c) Fourier spectrum of the modulation.

the wavevector is irrational. A shift of the phase α in eq. (5) gives rise to a displacement of the soliton lattice but its structure and energy remains unaffected. At the C–I transition the spacing l between solitons goes to infinity.

Figure 7 shows two high order C phases (also close to the $q = 1/4$ phase) formed by regular periodic soliton lattices. For C phases, the distance between two solitons is an integer number of lattice constants. The two soliton-lattices are slightly displaced relative to each other (the phases of the modulations differ by $\pi/2$). The two structures have different free energies so a C phase can, contrary to an I phase, not be displaced without changing the energy. The solitons are "pinned" to the lattice. The energy difference per soliton between the "pinned" and the "depinned" states (such as the two states on Fig. 7) is called the "pinning" energy. The energy of a soliton lattice (with period l) can be written [5]

$$F = E_{\text{sol}} \frac{1}{l} + E_{\text{int}} \frac{1}{l} \tag{7}$$

where the interaction energy is exponential

$$E_{\text{int}} \sim e^{-al}. \tag{8}$$

The transition from the C phase to an I phase takes place when the soliton energy E_{sol} becomes negative so that it becomes favorable to have solitons in the ground state. Figure 8 shows the free energy vs. soliton density, or wavenumber $q = (1/4) - (1/4l)$. The two dots for each high order C phase give the energies of the pinned and depinned solutions. The broken curve indicates that no one-dimensional trajectories representing I structures exist when the wavevector approaches $q = 1/4$, i.e. when the distance between solitons becomes too large. This is easy to understand in terms of the soliton picture. Figure 9 shows the pinning energy and the interaction energy (determined numerically) as a function of the soliton distance. For $l > l_c \sim 14$ lattice spacings the pinning energy exceeds the interaction energy. Hence, for $l > l_c$ the soliton lattice must necessarily be pinned to the crystal lattice, and the possibility of having an incommensurate phase with position independent energy ceases. The transition line beyond which there are no incommensurate phases is the analog of the line $K = 1$ for the circle map (see Fig. 2) beyond which there are no quasi-periodic orbits.

So, when the distance between the solitons becomes too large the interaction energy cannot overcome the pinning energy and all states must be pinned. When the pinned defects are regularly spaced the resulting state is high order commensurate. As the distances between the solitons are large they are effectively not interacting at all.

Extending the soliton picture a little further, one would expect stable states with a more or less *random* distribution of solitons on the lattice, since the weak interaction cannot possibly overcome the local pinning barriers. Indeed, such stable randomly pinned soliton states exist (Fig. 10(a)). These states appear as *chaotic* solutions to the four-dimensional map, eq. (4) (Fig. 10(b)). The distances between the solitons in the chaotic states are longer than the critical distance l_c for pinning of solitons [7]. The peaks in the spectrum $S(q)$ of the chaotic states have a finite width because of the disorder (Fig. 10(c)).

Although the chaotic states are stable the ordered states probably always have lower energy. If one accepts the picture involving exponentially decaying repulsion between solitons with constant pinning energy this can be shown rigorously [8]. A complete devil's staircase forms the ground state in the pinned regime. The chaotic states are much more abundant, however, and have essentially the same energy, so in an experiment one would expect to see a broadening of diffraction peaks caused by the metastable chaotic states. Figure 11 shows neutron diffraction measurements on the modulated magnetic system CeSb [9]. The peak position at low temperatures corresponds to a commensurate phase. At higher temperature the ordered state is incommensurate or high order commensurate. In between a broadening of the diffraction peak is observed. Mashiyama et al. [10] have observed a similar broadening near the CI transition in ferroelectric systems such as Rb_2ZnCl_4.

Thus, systems with competing spatial periods may exhibit spatially chaotic structures. The existence of these structures can easily be understood in terms of a picture involving randomly pinned defects and the structures can be identified experimentally. In some sense, the chaotic structures are the analogs of the intermittent chaotic orbits in dynamical systems, where periodic limit cycles are interrupted by irregularly spaced intermittent bursts.

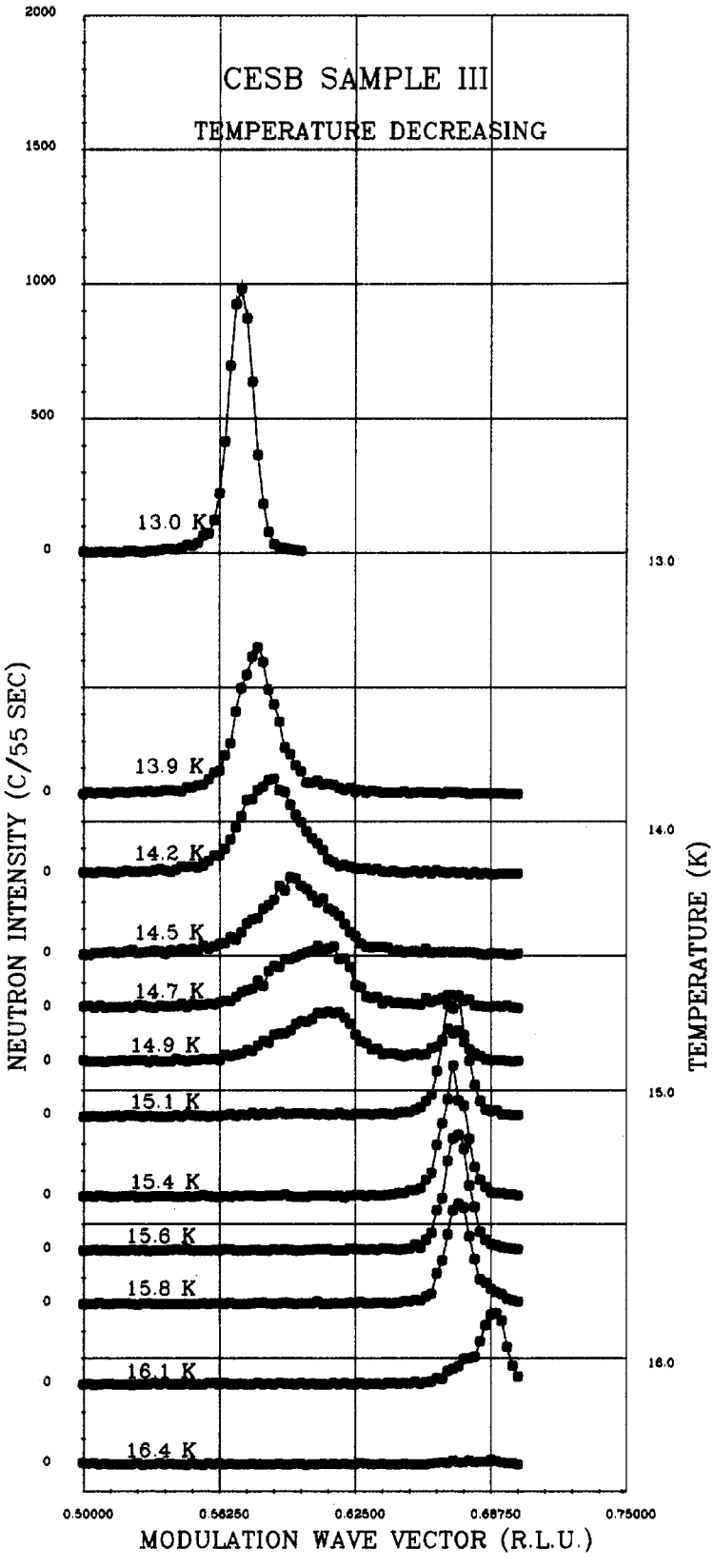

Fig. 11. Neutron diffraction measurements of $S(q)$ for cerium antimonide (CeSb) [9].

Acknowledgements

We are grateful to Bente Lebech for allowing us to present unpublished results as shown in Fig. 11. Work supported by Division of Materials Sciences, US DOE, under contract DE-AC02-76CH00016 and the Danish Natural Science Research Council.

References

1. Bak, P., Bohr, T. and Jensen, M. H., Physica Scripta **T9**, 000, 1984; Phys. Rev. Lett. **50**, 1637 (1983); Phys. Rev. A (in press).
2. Aubry, S., "Solitons and Condensed matter physics" (eds. A. Bishop and T. Schneider) p. 264, Springer, Berlin (1978).

3. Bak, P., Rep. Prog. Phys. **45**, 587 (1982).
4. Redner, S. and Stanley, H. E., J. Phys. **C10**, 4765 (1977); Fisher, M. E. and Selke, W., Phys. Rev. Lett. **44**, 1502 (1980); Villain, J. and Gordon, M., J. Phys. **C13**, 3117 (1980); Pokrovsky, V. L. and Uimin, G., J. Phys. **C15**, L353 (1982).
5. Bak, P. and von Boehm, J., Phys. Rev. **B21**, 5297 (1980).
6. Jensen, M. H. and Bak, P., Phys. Rev. **B27**, 6853 (1983); Phys. Rev. **B29**, 6280 (1984).
7. Bak, P. and Pokrovsky, V. L., Phys. Rev. Lett. **47**, 958 (1981).
8. Bak, P. and Bruinsma, R., Phys. Rev. Lett. **49**, 249 (1982); Phys. Rev. **B27**, 5824 (1983).
9. Lebech, B., Clausen, K. and Vogt, O. (to be published).
10. Mashiyama, H., Tanisaki, S. and Hamamo, K., J. Phys. Soc. Japan **50**, 2139 (1981).